Journal of Applied Polymer Science

Synthesis of Poly(amido amine)-Derived Dendrimers with Pendant Benzoxazine Groups and Their Thermal Behavior

Yanbing Lu, Junren Chen, Yunlong Lu, Pengbo Gai, Hailin Zhong
Institute of Polymer Research, College of Chemistry and Chemical Engineering, Hunan University, Changsha 410082, People's Republic of China

Correspondence to: Y. Lu (E-mail: yanbinglu@hnu.edu.cn)

ABSTRACT: Two novel dendrimer-derived compounds with pendant benzoxazine, named 0G benzoxazine (0G BOZ) and 1G benzoxazine (1G BOZ), were prepared using 0G poly(amido amine) (PAMAM) and 1G PAMAM, phenol, and paraformaldehyde. Effects of different generations of PAMAM on curing kinetics and thermal properties were investigated. Differential scanning calorimetric (DSC) measurements of the 0G BOZ and 1G BOZ were carried out at different heating rates of 5, 10, 15, and 20 K/min. Kinetic analysis by Kissinger's and Ozawa's method revealed the activation energy (E_a) of 0G BOZ were 109.1 and 109.3 kJ mol^{-1}, respectively, and those of 1G BOZ were 88.0 and 91.4 kJ mol^{-1}. The autocatalytic kinetic model was found to be the best description of the investigated curing reactions. In addition, the predicted curves from our kinetic models fit well with the nonisothermal DSC thermograms. Thermogravimetrical analysis of cured resin of 0G BOZ and 1G BOZ showed that the char yields of 0G BOZ and 1G BOZ were 37.6 and 26.3%, respectively. © 2012 Wiley Periodicals, Inc. J. Appl. Polym. Sci. 000: 000–000, 2012

KEYWORDS: dendrimers; synthesis; kinetics; benzoxazine; differential scanning calorimetry

Received 16 February 2010; accepted 12 April 2012; published online
DOI: 10.1002/app.37886

INTRODUCTION

Over the last decade, benzoxazines have attracted much attention of the research community because of their unique advantages over most of the known polymers. As a new kind of thermosetting phenolic resin, polybenzoxazines offer many excellent mechanical and physical properties, including high thermal stability, high T_g, high char yield, near zero volumetric shrinkage upon curing, low moisture absorption, and ability to be used as homopolymer, copolymer, and blends. They have recently been developed for the electronics, aerospace, and other industries as an attractive alternative to epoxies and traditional resole and novolac-type phenolic resins.[1–5]

Benzoxazines are six-membered heterocyclic compounds synthesized by the phenols, primary amines, and formaldehyde in solution or with a melt state reaction, so the wide variety of available phenolic and primary amines allows for tremendous opportunities in molecular design and imparts the ability to tailor the structure for specific applications. Great deals of researches were focused on synthesizing monofunctional and difunctional benzoxazine monomers.[6–12] However, the study of trifunctional and multifunctional benzoxazine monomers were few reported.[13–15]

Poly(amido amine) (PAMAM) dendrimers represent an exciting new class of macromolecular architecture called "dense star" polymers.[16–23] Unlike classical linear polymers, dendrimers have a high degree of molecular uniformity, narrow molecular weight distribution, specific size, and a highly functionalized terminal surface. PAMAM with lower generation can be thought of as flexible molecules with no appreciable inner regions. Herein, it is anticipated that the introduction of the flexible multiamines into the benzoxazine structure will bring some attractive features. With these objectives in mind, we explored the synthesis of PAMAM-based benzoxazine and investigated the properties of the resultant cured resin. In this article, 0G PAMAM with four terminal amine groups and 1G PAMAM with eight terminal amine groups were used as multiamine to synthesize multibenzoxazines. The effect of different generation PAMAM on the curing process and the thermal properties were also investigated via differential scanning calorimetry (DSC) and thermogravimetrical analysis (TGA).

EXPERIMENT

Material

Methyl acetate, dichloromethane, tetrahydrofuran, and chloroform were purchased from Sinopharm Chemical Reagent (Shanghai, China). Paraformaldehyde and phenol were

Applied Polymer SCIENCE

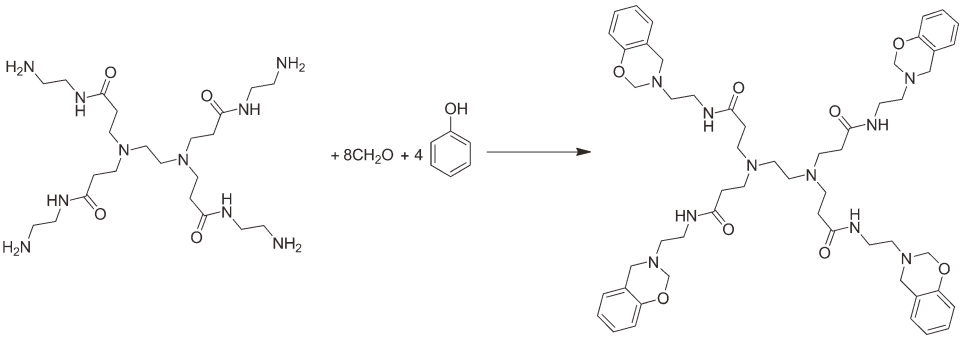

Scheme 1. Synthesis of 0G BOZ.

purchased from Tianjin Fuchen Chemicals Reagent Factory (Tianjin, China). All chemicals were used as received without further purification. 0G PAMAM and 1G PAMAM were synthesized according to the article reported.[16]

Measurements

Fourier transform infrared (FT-IR) spectrum was performed on a WQF-410 spectrophotometer (Beijing Second Optical Instrument Factory). Proton nuclear magnetic resonance (^{1}H NMR) spectra were recorded on an INOVA-400 instrument (Varian). The samples were dissolved in deuterated dimethylsulfoxide, and the solution was measured with tetramethylsilane as the internal reference.

DSC and TGA measurements were performed on a Netzsch STA 409 (Netzsch, Germany) under nitrogen atmosphere. The instrument was calibrated with a high-purity indium standard, and an empty cell was used as the reference. About 10 mg of sample was weighed into a hermetic aluminum sample pan at room temperature, which was then sealed, and the sample was tested immediately. The curing thermal data were obtained with different heating rates (5, 10, 15, and 20°C min^{-1}), heated from 30 to 400°C. The heat flow data, as a function of temperature and time, were obtained using the area under the peak of the exotherm. These data were processed further to obtain the fractional conversion and the rate of reaction.

Synthesis of 0G Benzoxazine

The solvent synthesis method was modified for the synthesis of tetrafunctional based benzoxazine monomer. 0G PAMAM, paraformaldehyde, and phenol were mixed in mole ratio about 1 : 8 : 16 in a three-neck round-bottom flask. Approximately, 5 mL of chloroform per gram of 0G PAMAM was added to the flask. The reaction mixture was refluxed with stirring for 5 h at 65°C. The crude products were filtered and dried under vacuum. The product was further purified by precipitated in ethyl acetate after dissolved in dichloromethane, then dried under vacuum at 60°C. The product was white powder after grinding. The theoretical molecular structure of 0G benzoxazine (0G BOZ) is given in Scheme 1.

Synthesis of 1G Benzoxazine

1G PAMAM, paraformaldehyde, and phenol were mixed in mole ratio about 1 : 16 : 32 in a three-neck round-bottom flask. Approximately 5 mL of chloroform per gram of 1G PAMAM was added to the flask. The reaction mixture was refluxed with stirring for 5 h at 65°C. The crude products were filtered, then the filtrate was concentrated and precipitated in ethyl acetate, and the product was further purified by tetrahydrofuran, then dried under vacuum. Products were white powder after grinding. The theoretical molecular structure of 1G benzoxazine (1G BOZ) is given in Scheme 2.

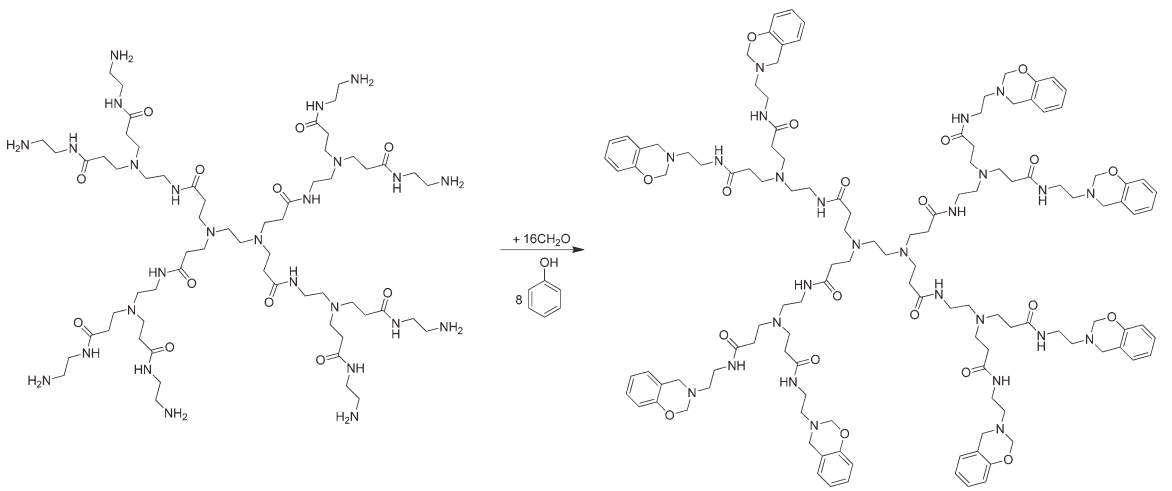

Scheme 2. Synthesis of 1G BOZ.

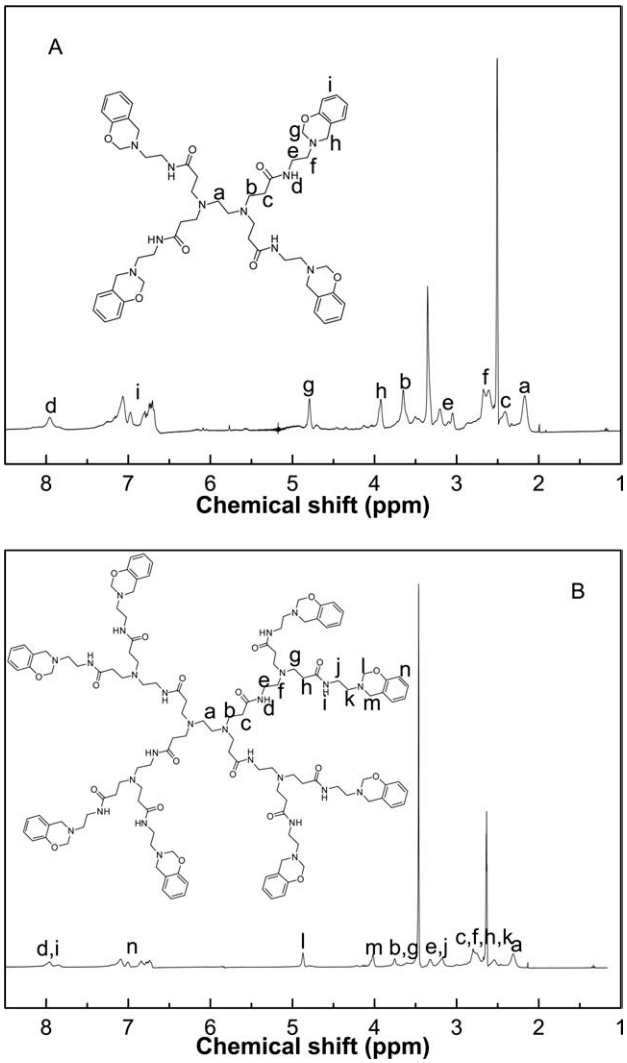

Figure 1. ^{1}H NMR spectra of 0G BOZ (A) and 1G BOZ (B).

RESULTS AND DISCUSSION

Characterization of Monomers

The ^{1}H NMR spectra of 0G BOZ and 1G BOZ are shown in Figure 1. Both spectra showed two peaks, centered at approximately 3.9 and 4.8 ppm, which were consistent with the formation of a benzoxazine ring, implying that the pendant benzoxazine groups were successfully synthesized. The disappearance peaks of 4.9 ppm (O—CH_2—N), 4.0 ppm (Ar—CH_2—N), and 3.0 ppm (CH_2—CH_2) showed the ethylene diamine-based benzoxazine monomer was completely removed by solvent precipitation method.[24]

The structure of 0G BOZ and 1G BOZ monomer was further confirmed by FT-IR. In Figure 2(A), the presence of cyclic ether of benzoxazine structure was confirmed by the absorbance peaks at 1034 and 1230 cm^{-1} due to the C—O—C symmetric stretching and asymmetric stretching modes, respectively. The characteristic peak of oxazine ring and acylamide group (O=C—NH) were located at 931 and 1653 cm^{-1}, respectively. The peak at 1365 cm^{-1} was assigned to CH_2 wagging. The absorption bands

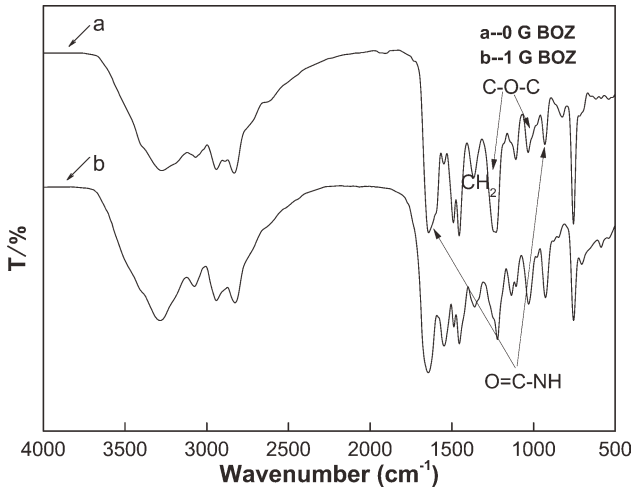

Figure 2. FT-IR spectra of the 0G BOZ (a) and 1G BOZ (b).

characteristic of *ortho*-disubstituted benzene appeared at 756 cm^{-1}. In Figure 2(B), the C—O—C symmetric stretching and asymmetric stretching modes were located at 1030 and 1221 cm^{-1}, respectively, and the characteristic peak of oxazine ring was located at 928 cm^{-1}, FT-IR data of the 1G BOZ were similar to 0G BOZ attribute to the homologous structure they have.

As shown in Figure 3, open loop process of the oxazine ring at different temperatures during curing was observed. A cure profile (150°C/2 *h*, 200°C/2 *h*, and 240°C/2 *h*) was applied for the curing of the 0G BOZ monomer. The curves b, c, and d were corresponding to the different temperatures in curing. With enhancing the curing temperature, oxazine ring was open to produce a phenolic hydroxyl group, the absorption intensity of the peak enhanced gradually from 3290 to 3390 cm^{-1}. Previous research showed that hydrogen bonding of the hydroxyl group played an important role in the network structure of polybenzoxazines and may contribute to many of their physical and mechanical properties.[24] From a to d, the absorption of the peak(O=C—NH) decreased gradually from 1653 to 1604 cm^{-1}

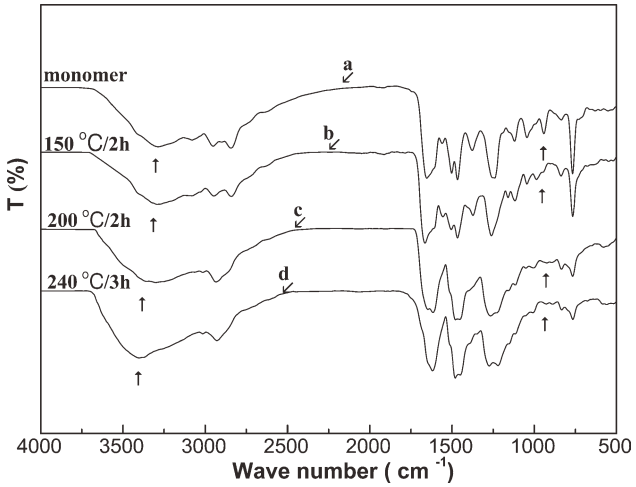

Figure 3. FT-IR spectra of the 0G BOZ after each cure stage.

Applied Polymer SCIENCE

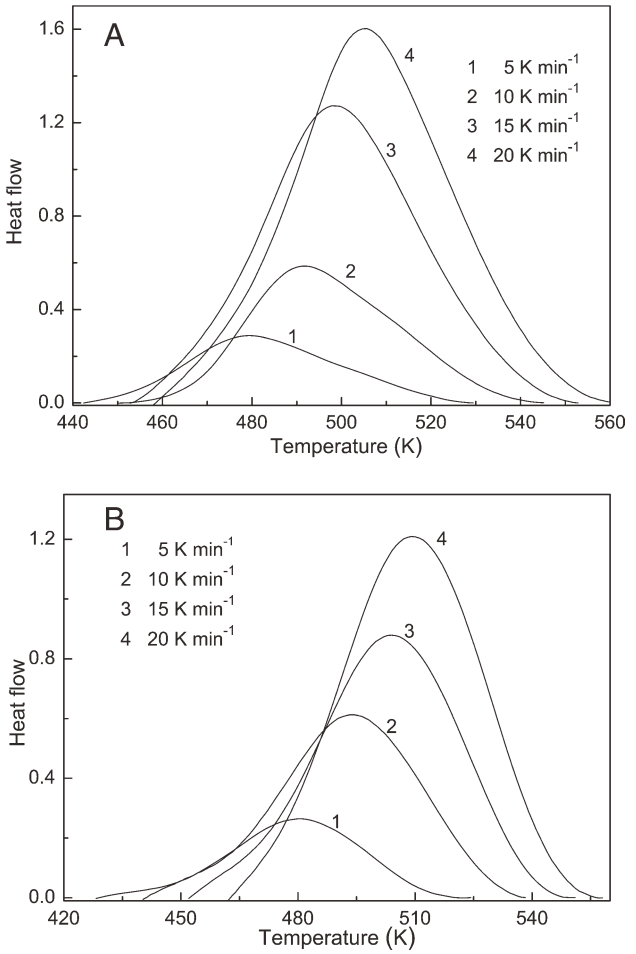

Figure 4. Dynamic DSC thermograms of the 0G BOZ (A) and 1G BOZ (B).

along with the increasing of the hydroxyl groups, because the carbonyl group and hydroxyl group formed hydrogen bonding. According to the oxazine rings reducing with curing, the absorption intensity of the peak at 931 cm^{-1} decreased. The absorption at 754 and 822 cm^{-1} showed the presence of the expected *ortho*-substituted benzene rings after curing.

Curing Behavior of the Monomers

The curing behavior of the two monomers was studied by DSC. Figures 4 and 5 show the DSC thermograms and the conversion versus temperature at different heating rates. From Figure 4, information about the nature of the curing reaction such as initial curing temperature (T_i), peak temperature (T_p), and the curing range at different heating rates could be derived. It can be observed that the increase of heating rate leads to decrease of the cure time, and the exothermic peak shifts to a higher temperature with higher heating rate. The T_i and T_p values were lower than those monobenzoxazine derived from cresol and aniline[25] and dibenzoxazine derived from bisphenol A and aniline,[26] indicating that the flexible inner PAMAM core could improve the curing of the benzoxazine. The T_i of 1G BOZ was lower than that of OG BOZ at the same heating rate, which was due to the molecular mobility of the benzoxazine group. But the T_p of the two monomers at same heating rate did not show much difference because of the nature of ring opening of benzoxazine ring.

Generally, the apparent activation energy E_a can be calculated using the well-known methods for dynamic heating experiment, Kissinger method and Ozawa method.[27,28]

Kissinger method is based on the fact that exothermic peak temperature T_p varies with the heating rates, and it assumes that the maximum reaction rate occurs at the peak temperatures. The equation can be expressed as eq. (1):

$$\ln(\beta/T_p^2) = \ln(AR/E_a) - E_a/(RT_p) \quad (1)$$

where β is the heating rate, A the frequency factor, and R the universal gas constant.

If the plot of $\ln(\beta/T_p^2)$ against $1/T_p$ is linear, the E_a can be obtained from the slope of the corresponding straight line.

Another theoretical treatment, namely, the Ozawa method, can be also applied to the thermal data, using the following eq. (2):

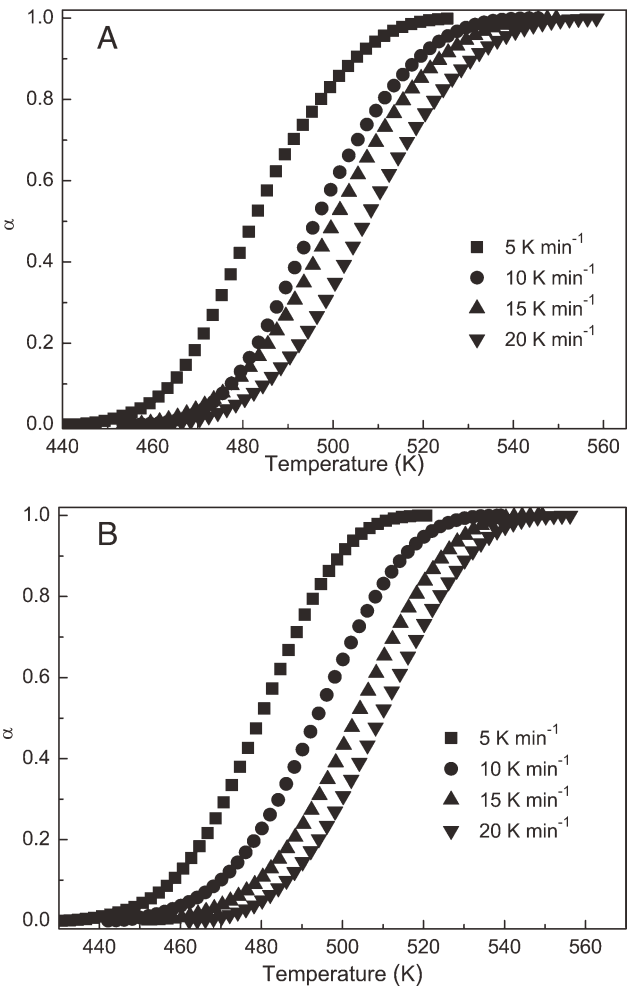

Figure 5. Conversion as a function of cure temperature of the 0G BOZ (A) and 1G BOZ (B).

Table I. Activity Energy Values of 0G BOZ and 1G BOZ Obtained from Kissinger and Ozawa Methods

		E_a	R^2
0G BOZ	Kissinger method	109.1 ± 2.1	0.9956
	Ozawa method	109.3 ± 0.3	0.9999
1G BOZ	Kissinger method	88.0 ± 1.4	0.9967
	Ozawa method	91.4 ± 1.3	0.9973

$$\ln \beta = -5.331 - 1.052\left(\frac{E_a}{RT_p}\right) + \ln\left(\frac{AE_a}{R}\right) - \ln f(\alpha) \quad (2)$$

It is on the assumption that the degree of conversion at peak temperatures for different heating rates is constant. Thus, at the same conversion, the plot of ln β versus $1/T_p$ should be a straight line with the slope of 1.052 E_a/R.

The E_a values of 0G BOZ and 1G BOZ calculated by Kissinger and Ozawa method are listed in Table I. The E_a values of 0G BOZ are 109.1 and 109.3 kJ mol^{-1}, respectively, according to Kissinger and Ozawa method. And the E_a values of 1G BOZ are 88.0 and 91.4 kJ mol^{-1}. The E_a values from Kissinger and Ozawa method were quite close to each other, and their differences may be caused by the different assumptions. An interpretation of the lower E_a values of 1G BOZ is an apparent increase in molecular mobility of the benzoxazine group during the curing process. The E_a values of the multifunctional benzoxazine were lower than those monobenzoxazine derived from cresol and aniline,[25] further implied that the PAMAM core can improve the thermal curing of the resin.

Curing Kinetic Model

To examine the kinetic model, it is necessary to appeal to the special functions $y(\alpha)$ and $z(\alpha)$.[29,30]

$$y(\alpha) = \left(\frac{d\alpha}{dt}\right)e^x \quad (3)$$

$$z(\alpha) = \pi(x)\left(\frac{d\alpha}{dt}\right)\frac{T}{\beta} \quad (4)$$

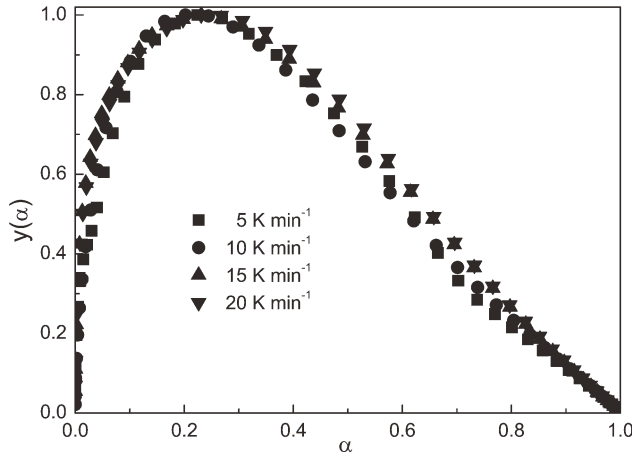

Figure 6. Variation of $y(\alpha)$ function versus conversion of the 0G BOZ.

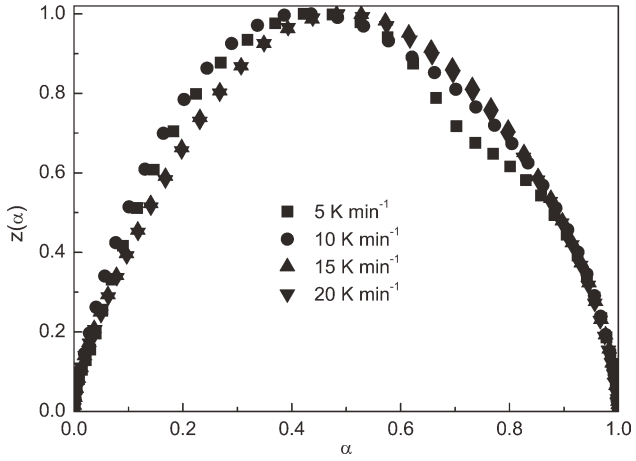

Figure 7. Variation of $z(\alpha)$ function versus conversion of the 0G BOZ.

where x is reduced activation energy (E_a/RT), β the heating rate, T absolute temperature, and $\pi(x)$ is the expression of the temperature integral. In our study, the activation energy value obtained from Kissinger method was used. As was pointed out, $\pi(x)$ function can be well approximated using the fourth rational expression of Senum and Yang[31] as in eq. (5)

$$\pi(x) = \frac{x^3 + 18x^2 + 88x + 96}{x^4 + 20x^3 + 120x^2 + 240x + 120} \quad (5)$$

For practical reasons, the $y(\alpha)$ and $z(\alpha)$ functions are normalized within (0,1) range. Figures 6 and 7 show the variation of $y(\alpha)$ and $z(\alpha)$ values with conversion of 0G BOZ. These functions exhibit maxima at α_M and α_p^∞, respectively. Both α_M and α_p^∞ help to decide the choice of the kinetic model.[29,30]

Table II lists the values of maxima α_M and α_p^∞ corresponding to the functions $y(\alpha)$ and $z(\alpha)$, together with α_p taken as the maximum of the DSC peak. It can be seen that α_M, α_p^∞, and α_p values were independent with the heating rate. And the values of α_M were lower against the value of α_p, whereas α_p^∞ exhibits values lower than 0.632 (a characteristic value for the kinetic model determination).[32] These remarks indicated that the studied curing process can be described using the two parameter autocatalytic kinetic model Šesták-Berggren [eq. (6)].[33]

Table II. Values of α_p, α_M, and α_p^∞ for 0G BOZ and 1G BOZ Obtained from DSC Thermograms Analysis

Heating rate (°C min^{-1})	0G BOZ			1G BOZ		
	α_p	α_M	α_p^∞	α_p	α_M	α_p^∞
5	0.42	0.22	0.42	0.52	0.18	0.57
10	0.44	0.24	0.44	0.51	0.20	0.56
15	0.48	0.23	0.48	0.52	0.18	0.52
20	0.48	0.23	0.48	0.48	0.17	0.52

Table III. The Kinetic Parameters Evaluated for 0G BOZ and 1G BOZ

	Heating rate (°C min^{-1})	E_a (kJ mol^{-1})	ln A (s^{-1})	Mean	n	Mean	m	Mean	R
0G BOZ	5	109.1	26.8	26.6	1.89	1.74	0.46	0.39	0.9992
	10		26.6		1.91		0.41		0.9998
	15		26.5		1.60		0.33		0.9995
	20		26.4		1.54		0.35		0.9984
1G BOZ	5	88.0	21.1	21.1	1.30	1.29	0.37	0.36	0.9979
	10		21.1		1.33		0.38		0.9985
	15		21.0		1.25		0.36		0.9986
	20		21.1		1.26		0.34		0.9994

$$f(\alpha) = (1-\alpha)^n \alpha^m \tag{6}$$

where m and n are the kinetic exponents.

Thus, the reaction rate can be described as follows:

$$\frac{d\alpha}{dT} = \frac{A}{\beta}\exp\left(-\frac{E_a}{RT}\right)(1-\alpha)^n \alpha^m \tag{7}$$

Theoretically, eq. (7) could be solved by multiple nonlinear regressions, because the curing rate is an exponential function of the reciprocal of the absolute temperature. By taking the natural logarithm of eq. (7), a linear expression for the natural logarithm of curing rate can be obtained:

$$\ln\left(\beta\frac{d\alpha}{dT}\right) = -\frac{E_a}{RT} + n\ln(1-\alpha) + m\ln(a) + \ln A \tag{8}$$

Equation (8) can be solved by multiple linear regression, in which the dependent variable is $\ln(d\alpha/dt)$, and the independent variables are $1/T$, $\ln(1-\alpha)$, and $\ln(\alpha)$. Therefore, the values of A, m, and n can be obtained using the average activation energy from Kissinger method. The degree of curing is chosen between the beginning of the reaction and the maximum peak of degree of curing (α = 0.1–0.5). The kinetic parameters evaluated for the proposed Šesták-Berggren kinetic model are listed in Table III.

The correctness of the kinetic model proposed using the Šesták-Berggren equation was verified. The experimental curves and calculated curves at different heating rates are shown in Figure 8. It is clearly seen that the calculated data from the model are in good agreement with the experimental results. This means that the two parameter Šesták–Berggren model gives a good description of the curing process.

TGA Analysis

The thermal stability of 0G BOZ and 1G BOZ were studied by TGA. Figure 9 shows the TGA thermograms of both 0G BOZ and 1G BOZ. The 5% and 10% weight loss temperatures (designated as Td_5 and Td_{10}) for 0G BOZ were 265.4°C and 313.5°C, whereas for 1G BOZ, Td_5 and Td_{10} were 221.8°C and 304.1°C. The char yield, as defined as the weight residue remaining at 800°C under nitrogen atmosphere, of 0G BOZ was 37.6%, and that of 1G BOZ was 26.3%. Compared with the 0G PAMAM, the Td_5, Td_{10}, and char yield of 0G BOZ enhanced largely, which can be attributed to crosslinking due to the importing of benzoxazine group. However, Td_5, Td_{10}, and char yield of 1G BOZ were lower than those of 0G BOZ, which was not unexpected considering that as the PAMAM content is being

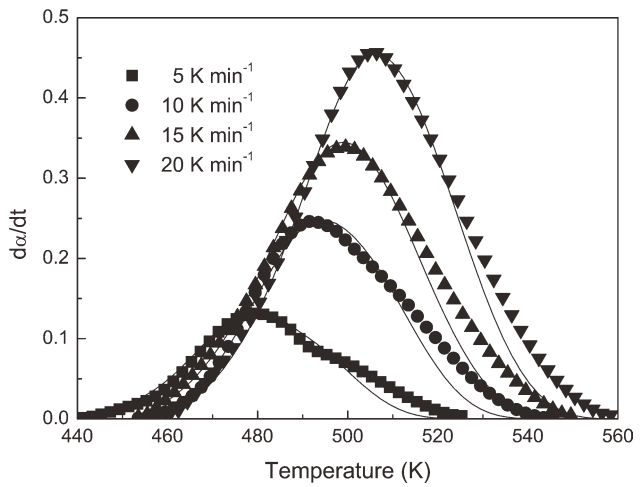

Figure 8. Experimental (symbols) and calculated (solid lines) DSC peaks corresponding to the curing process of 0G BOZ.

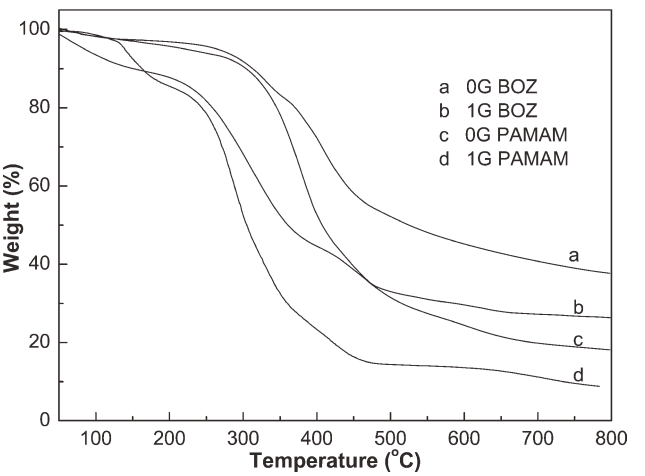

Figure 9. TGA curves of 0G BOZ (a), 1G BOZ (b), 0G PAMAM (c), and 1G PAMAM (d).

increased, aromatic content should inversely decrease. The same tendency was also observed in the aliphatic diamine-based benzoxazine system. As the chain length of the aliphatic diamine increased, the Td_5 and char yield decreased.[34]

Char yield can be used as a criterion for evaluating limiting oxygen index (LOI) of the resins in accordance with Van Krevelen and Hoftyzer equation.[35]

$$\mathrm{LOI} = 17.5 + 0.4\ \mathrm{CR} \quad (9)$$

where CR is the char yield.

Based on the char yield, the LOI values of the 0G BOZ and 1G BOZ were 32.5 and 28.0, respectively, implying that they could be classified as self-extinguishing materials.

CONCLUSIONS

Dendrimer-derived benzoxazine monomers were prepared from 0G PAMAM and 1G PAMAM via solution method. Cure kinetics of 0G BOZ and 1G BOZ were investigated by DSC at the different heating rates. The activation energy of the 1G BOZ was lower than that of 0G BOZ because of the increase in molecular mobility of the benzoxazine group during the curing process. The autocatalytic kinetic model was found to be the best description of the investigated curing reactions. Evidently, the kinetic models of the curing reaction were in good agreement with nonisothermal DSC results. TGA result showed that the prepared benzoxazine had the excellent thermal stability. The Td_5 of 0G BOZ and 1G BOZ were 265.4°C and 221.8°C, while the char yield 37.6% and 26.3%, respectively. Incorporation of the benzoxazine groups resulted in higher thermal stability of the PAMAM and higher generation PAMAM could decrease the thermal properties of the obtained benzoxazine.

ACKNOWLEDGMENTS

The authors gratefully acknowledge the financial support of the Natural Science Foundation of Hunan Province, China (Grant No. 09JJ5009).

REFERENCES

1. Chutayothin, P.; Ishida, H. *Eur. Polym. J.* **2009,** *45*, 1493.
2. Allen, D. J.; Ishida, H. *Polymer* **2009,** *50*, 613.
3. Santhosh Kumar, K. S.; Reghunadhan Nair, C. P.; Ninan, K.N. *Eur. Polym. J.* **2009,** *45*, 494.
4. Chernykh, A.; Agag, T.; Ishida, H. *Polymer* **2009,** *50*, 382.
5. Ishida, H.; Lee, Y. H. *Polymer* **2001,** *42*, 6971.
6. Goward, G. R.; Sebastiani, D., Schnell, I.; Spiess, H. W.; Kim, H. D.; Ishida, H. *J. Am. Chem. Soc.* **2003,** *125*, 5792.
7. Laobuthee, A.; Chirachanchai, S.; Ishida, H.; Tashiro, K. *J. Am. Chem. Soc.* **2001,** *123*, 9947.
8. Kim, H. D.; Ishida, H. *Macromolecules* **2003,** *36*, 8320.
9. Lu, Y. B.; Li, M. M.; Zhang, Y. J.; Hu, D.; Ke, L. L.; Xu, W. *J. Thermochim. Acta* **2011,** *515*, 32.
10. Zhong, H. L.; Lu, Y. B.; Chen, J. R.; Xu, W. J.; Liu, X. *J. Appl. Polym. Sci.* **2010,** *118*, 705.
11. Ishida, H.; Sanders, D. P. *Macromolecules* **2000,** *33*, 8149.
12. Agag, T.; Takeichi, T. *Macromolecules* **2003,** *36*, 6010.
13. Subrayan, R. P.; Jones, F. N. *Chem. Mater.* **1998,** *10*, 3506.
14. Ghosh, N. N.; Kiskan, B.; Yagci.Y. *Prog. Polym. Sci.* **2007,** *32*, 1344.
15. Zhang, J.; Xu, R. W.; Yu, D. S. *Eur. Polym. J.* **2007,** *43*, 743.
16. Tomalia, D. A.; Baker, H.; Dewald, J.; Hall, M.; Kallos, G.; Martin, S.; Roeck, J.; Ryder, J.; Smith, P. *Polym. J.* **1985,** *17*, 117.
17. Matthews, O. A.; Shipway, A. N.; Stoddard, J. F. *Prog. Polym. Sci.* **1998,** *23*, 1.
18. Nourse, A.; Millar, D. B.; Minton, A. P. *Biopolymer* **2000,** *53*, 316.
19. Jackson, C. L.; Chanzy, H. D.; Booy, F. P.; Drake, B. J.; Tomalia D. A.Bauer, B. J.; Amis, E. *J. Macromolecules* **1998,** *31*, 6259.
20. Newkome, G. R.; Shreiner, C. D. *Polymer* **2008,** *49*, 1.
21. Tomalia, D. A.; Frechet, J. M. J. *J. Polym. Sci. Part A: Polym. Chem.* **2002,** *40*, 2719.
22. Tomalia, D. A.; Majoros, I. *J. Macromol. Sci. Polym. Rev.* **2003,** *43*, 411.
23. TomaliaD.A. *Soft Matter.* **2010,** *6*, 456.
24. Allen, D. J.; Ishida, H. *Polymer* **2007,** *48*, 6763.
25. Huang, J. X.; Zhang, J.; Wang, F.; Huang, F. R.; Du, L. *React. Funct. Polym.* **2006,** *66*, 1395.
26. Ishida, H.; Rodriguez, Y. *Polymer* **1995,** *36*, 3151.
27. Kissinger, H. E. *J. Annu. Chem.* **1957,** *29*, 1702.
28. Ozawa, T. *J. Therm. Anal.* **1970,** *2*, 301.
29. Malek, J. Thermochim. *Acta* **2000,** *355*, 239.
30. Malek, J. Thermochim. *Acta* **1992,** *200*, 257.
31. Senum, G. I.; Yang, R. T. *J. Therm. Anal.* **1977,** *11*, 445.
32. Montserrat, S.; Malek, *J. Thermochim. Acta* **1993,** *228*, 47.
33. Šesták, C.; Berggren, G. *Thermochim. Acta* **1971,** *3*, 1.
34. Allen, D. J.; Ishida, H. *J. Appl. Polym. Sci.* **2006,** *101*, 2798.
35. Vankrevelen, D. W.; Hoftyzer, P. J. Properties of Polymers; Elsevier: New York, **1976;** p 529.